The current issue and full text archive of this journal is available at
www.emeraldinsight.com/0961-5539.htm

A fully explicit three-step SPH algorithm for simulation of non-Newtonian fluid flow

S.M. Hosseini, M.T. Manzari and S.K. Hannani
Center of Excellence in Energy Conversion, School of Mechanical Engineering, Sharif University of Technology, Tehran, Iran

Received 19 February 2006
Reviewed 30 July 2006
Accepted 7 September 2006

Abstract

Purpose – This paper sets out to present a fully explicit smoothed particle hydrodynamics (SPH) method to solve non-Newtonian fluid flow problems.

Design/methodology/approach – The governing equations are momentum equations along with the continuity equation which are described in a Lagrangian framework. A new treatment similar to that used in Eulerian formulations is applied to viscous terms, which facilitates the implementation of various inelastic non-Newtonian models. This approach utilizes the exact forms of the shear strain rate tensor and its second principal invariant to calculate the shear stress tensor. Three constitutive laws including power-law, Bingham-plastic and Herschel-Bulkley models are studied in this work. The imposition of the incompressibility is fulfilled using a penalty-like formulation which creates a trade-off between the pressure and density variations. Solid walls are simulated by the boundary particles whose positions are fixed but contribute to the field variables in the same way as the fluid particles in flow field.

Findings – The performance of the proposed algorithm is assessed by solving three test cases including a non-Newtonian dam-break problem, flow in an annular viscometer using the aforementioned models and a mud fluid flow on a sloping bed under an overlying water. The results obtained by the proposed SPH algorithm are in close agreement with the available experimental and/or numerical data.

Research limitations/implications – In this work, only inelastic non-Newtonian models are studied. This paper deals with 2D problems, although extension of the proposed scheme to 3D is straightforward.

Practical implications – This study shows that various types of flow problems involving fluid-solid and fluid-fluid interfaces can be solved using the proposed SPH method.

Originality/value – Using the proposed numerical treatment of viscous terms, a unified and consistent approach was devised to study various non-Newtonian flow models.

Keywords Hydrodynamics, Materials handling, Flow, Viscosity

Paper type Research paper

1. Introduction

Production and processing of Rheologically complex materials is a thriving industry which deals with many millions of tones of materials per year. Examples of such materials can be found in the case of solutions and melts of macro-molecules, that is, polymeric materials and biological systems. Processes for manufacturing of coated sheets, optical fibers and plastics are amongst other examples. Obviously, a better understanding of the physical and mechanical behavior of such materials is essential to devise efficient production methods and economical manufacturing procedures.

There has been a tremendous amount of research in response to demand for characterization, modeling and simulation of rheological materials (Baaijens, 1998; Bingham, 1922; Bird *et al.*, 1987; Owens and Phillips, 2002). An important class of

International Journal of Numerical Methods for Heat & Fluid Flow
Vol. 17 No. 7, 2007
pp. 715-735

0961-5539
DOI 10.1108/09615530710777976

non-Newtonian fluids is represented by the so-called inelastic models which describe a large group of complex materials. Three examples of this model are the power-law, Herschel-Bulkley and Bingham-plastic models. In these models, viscosity is a function of invariants of deformation-rate tensor. From a numerical point of view, a challenging feature of these models is their multi-valued behavior. Flows of such fluids exhibit regions of plug flow and inelastic flow with large shear deformation. Below a particular yield stress, local shear rates are zero with no fluid deformation. When the local stress exceeds the yield stress, the fluid undergoes deformation. In this case, a yield surface separates the solid-like plug flow and the viscous flow regions. A simple treatment of such fluids is achieved by using a bi-viscosity model. Unlike the theoretical behavior, however, the bi-viscosity model allows fluid motion or yielding even below the yield point. An alternative to the bi-viscosity model is to solve for the shape of the yield surface together with velocity and pressure fields in the fluid portion of the material.

In recent years, significant progress has been made in the context of computational rheology. Several numerical methods have been devised to study non-Newtonian fluid flows with different degrees of success (Bose and Carey, 1999; Matallah *et al.*, 2002; Webster *et al.*, 2004; Vola *et al.*, 2004; Renardy, 2000). More specifically, Galerkin finite element methods have been used for analysis of Bingham-plastic fluids but exhibit appreciable errors in the calculated shear rates and viscosities (Bose and Carey, 1999). These methods also require satisfaction of the LBB consistency condition which places a restriction on the stress approximation space in non-Newtonian flows and increases computational cost. Moreover, in shear-thinning inelastic models like the power-law model, local viscosity may reduce significantly resulting in high-mesh Reynolds numbers for some elements and eventually unstability in the solution.

A viable numerical method for solving fluid flow problems is the so-called smoothed particle hydrodynamics (SPH) method. The method uses a purely Lagrangian approach and has been successfully employed in a wide range of problems. The SPH method is a branch of meshless methods and unlike conventional Eulerian methods does not use a fixed grid to represent the computational domain. That is the method does not require connectivity data as needed by the finite volume and finite element methods. This gives the method a very useful feature when dealing with complex flows exhibiting large deformations and/or free-surfaces. Another useful feature of the method is that its extension to 3D problems is particularly simple (Owen, 2004).

The SPH method is a particle-based method. The word "particle" does not mean a physical mass, instead, it refers to a region in space. Field variables are associated to these particles and at any other point in space are found by averaging, or smoothing, the particle values over the region of interest. This is fulfilled by an interpolation or weight function which is often called the interpolation kernel (Chaniotis *et al.*, 2002).

The SPH method was originally developed by Lucy (1977) and Gingold and Monaghan (1977) to solve compressible astrophysical problems. The method was later extended to incompressible flows by Monaghan (1994) and Takeda *et al.* (1994). Several other researchers have since contributed to the method and solved various engineering problems including heat transfer (Chaniotis *et al.*, 2002; Cleary *et al.*, 2002), turbulent flows (Welton, 1998), interfacial flows (Colagrossi and Landrini, 2003) and sloshing (Kelecy and Fletcher, 1997; Koshizuka *et al.*, 1995) problems.

An important aspect of solving incompressible flows using SPH is the way it handles the incompressibility. There are various approaches to incorporate the incompressibility

in SPH methods. One approach termed as "weakly compressible" solves the incompressible flow as a compressible flow but with a very small Mach ($M \approx 0.1$) number. This approach has acceptable results in flows with low-Reynolds number, but errors increase un-acceptedly in fully confined moderate and high-Reynolds number flows (Cummins and Rudman, 1999). Another approach which works for high-Reynolds number flows is the particle method proposed by Koshizuka *et al.* (1995). In this approach, a penalty-like formulation is employed to adjust the pressure where density variations occur. An iterative process is used until density variations become less than a specified tolerance. A similar approach was used in Koshizuka *et al.* (1998), where instead of a penalty method, a pressure Poisson equation was solved with a source term proportional to density variations.

Only recently non-Newtonian flows were investigated using the SPH methods. Ellero *et al.* (2002) developed a numerical scheme based on the SPH method to study viscoelastic fluid flows using a Maxwell model. Also, Shao and Lo (2003) presented a SPH method to solve non-Newtonian flows with free surfaces using a modified form of the so-called cross model.

In this paper, a new SPH algorithm is presented to solve non-Newtonian fluid flow problems. The method is fully explicit in time and uses a three-step algorithm. An approach similar to the traditional Eulerian-based methods is adopted for computing viscous terms facilitating the description of non-Newtonian constitutive laws in SPH. Below, first a brief description of the SPH method is given and various related numerical issues are discussed. Then, the treatment of viscous terms particularly when non-Newtonian fluid flows are studied is given. Three non-Newtonian models including power-law, Herschel-Bulkley and Bingham-plastic models are described and their implementation in a SPH context is elaborated. Finally, three test cases are solved to demonstrate the performance of the proposed algorithm. The first test case is a non-Newtonian dam-break problem. The second test case deals with flow in a viscometer using different non-Newtonian models and the third test case investigates a laminar non-Newtonian flow of mud on a mild slope.

2. Fundamentals

The SPH method is based on the interpolation theory. The method allows any function to be expressed in terms of its values at a set of disordered points representing particle positions using a kernel function. The kernel function refers to a weighting function and specifies the contribution of a typical field variable, $A(r)$, at a certain position, r, in space. The kernel estimate of $A(r)$ is defined as (Monaghan, 1992):

$$< A_h(\mathbf{r}) >= \int_V A(\mathbf{r}')W(\mathbf{r} - r', h)\mathrm{d}\mathbf{r}' \tag{1}$$

where V represents the solution space, the smoothing length h represents the effective width of the kernel and W is a weighting function with the following properties:

$$\int_V W(\mathbf{r} - r', h)\mathrm{d}\mathbf{r}' = 1 \quad \lim_{h\to 0} W(\mathbf{r} - r', h) = \delta(\mathbf{r} - r') \tag{2}$$

If $A(\mathbf{r}')$ is known only at a discrete set of N point $\mathbf{r}_1, \mathbf{r}_2, \ldots \mathbf{r}_N$,, then $A(\mathbf{r}')$ can be approximated as follows (Monaghan, 1992):

$$A(\mathbf{r}') = \sum_{j=1}^{N} \delta(\mathbf{r}' - \mathbf{r}_j) A(\mathbf{r}_j)(\mathrm{d}V)_j \tag{3}$$

where $(\mathrm{d}V)_j$ is the differential volume element around the point r_j. Combining equations (1) and (3) yields (Schlatter, 1999):

$$< A_h(\mathbf{r}) >= \sum_{j=1}^{N} \int \delta(\mathbf{r}' - r_j) A(\mathbf{r}_j)(\mathrm{d}V)_j W(\mathbf{r} - r', h)\mathrm{d}\mathbf{r}' \tag{4}$$

After integration, and replacing the differential volume element $(\mathrm{d}V)_j$ by m_j/ρ_j one gets (Schlatter, 1999):

$$< A_h(\mathbf{r}) >= \sum_{j=1}^{N} \frac{m_j}{\rho_j} A_j W(\mathbf{r} - \mathbf{r}_j, h) \tag{5}$$

where the summation index j denotes a particle label and particle j carries a mass m_j at position $\mathbf{r}_j$, a density ρ_j and a velocity $\mathbf{v_j}$. The value of A of j-th particle is shown by A_j. The summation is over particles which lie within a circle of radius $2h$ centered at $\mathbf{r}$.

2.1 Kernel function

The kernels used in the SPH method approximate a δ function. Monaghan (1992) suggests that a suitable kernel must have a compact support in order to ensure zero interactions outside its computational range. The original calculations of Gingold and Monaghan (1977) used a Gaussian kernel. Although this kernel satisfies the basic requirements given by equation (2), it does not possess a compact support so its computational efficiency is rather low (Hongbin and Xin, 2004). Various forms with a compact support such as super-Gaussian (Monaghan and Gingold, 1983), spline (Monaghan, 1985), polynomial (Gingold and Monaghan, 1982) and cosine (Fulk and Quinn, 1996) kernels were proposed later. Recent studies (Monaghan, 1992; Morris *et al.*, 1997) indicate that the stability of the SPH algorithm depends strongly upon the second derivative of the kernel. A kernel must be able to minimize the errors caused by using the interpolation method. Monaghan (1992) analyzed the estimation errors of the method and stated that the errors are proportional to h^2 when the kernel is an even function of x, and to h^4 when the kernel satisfies the following relation (Hongbin and Xin, 2004):

$$\int x^2 W(x, h)\mathrm{d}x = 0 \tag{6}$$

One of the most popular kernels is based on spline functions (Monaghan, 1992) as defined by:

$$W(r, h) = \frac{\sigma}{h^m} \times \begin{cases} 1 - \frac{3}{2}s^2 + \frac{3}{4}s^3 & 0 \le s < 1 \\ \frac{1}{4}(2 - s)^3 & 1 \le s < 2 \\ 0 & 2 \le s \end{cases} \tag{7}$$

Here, $s = |\mathbf{r}|/h$, m represents the number of dimensions and σ is a normalization constant which takes the values 2/3, $10/7\pi$, $1/\pi$ in one, two and three dimensions, respectively.

This kernel has compact support so that its interactions are exactly zero for $r > 2h$. The first and second derivatives of this kernel are continuous implying that the interpolation is not too sensitive to particle disorder. Also, the latter property means that the dominant error term in the integral interpolant is $O(h^2)$. Higher-order splines can be used, but they interact with further particles and thus require more computational time.

It should be added that the SPH methods work best when the number of neighboring particles is between 20 and 30 in 2D cases. One way to maintain this number is to adjust the smoothing length of the particles dynamically. It is also vital to use the same smoothing length when calculating the forces exchanged between two neighboring particles, say i and j. Otherwise, the conservation of momentum is violated. In SPH, it is common to compute the smoothing length associated with particles i and j according to $h_{ij} = (h_i + h_j)/2$ where h_i and h_j may be calculated using an appropriate rule described in Schlatter (1999).

2.2 Gradient and divergence

The gradient and divergence operators need to be formulated in a SPH algorithm if simulation of the Navier-Stokes equations is to be attempted. In this work, the following commonly used forms are employed for gradient of a scalar A and divergence of a vector $\mathbf{u}$ (Colagrossi and Landrini, 2003):

$$\frac{1}{\rho_i}\nabla_i A = \sum_j m_j \left(\frac{A_i}{\rho_i^2} + \frac{A_j}{\rho_j^2}\right)\nabla_i W_{ij} \tag{8}$$

$$\frac{1}{\rho_i}\nabla_i \cdot \mathbf{u}_i = \sum_j m_j \left(\frac{\mathbf{u}_i}{\rho_i^2} + \frac{\mathbf{u}_j}{\rho_j^2}\right)\nabla_i W_{ij} \tag{9}$$

where $\nabla_i W_{ij}$ is gradient of the kernel function $W(|\mathbf{r}_i - \mathbf{r}_j|, h)$ with respect to $\mathbf{r}_i$, the position of particle i. This choice of discretization operators ensure that an exact projection algorithm is produced. There are a number of different ways of representing these operators some of which proven to be more convenient in terms of accuracy and robustness of the method (Bonet and Lok, 1999).

2.3 Laplacian formulation

A simple way to formulate the Laplacian operator is to envisage it as dot product of the divergence and gradient operators. This approach proved to be problematic as the resulting second derivative of the kernel is very sensitive to particle disorder and when dealing with the Navier-Stokes equations can easily lead to pressure instability and decoupling in the computation due to the co-location of the velocity and pressure. In this paper, the following alternative approach is adopted (Cummins and Rudman, 1999):

$$\nabla\left(\frac{1}{\rho}\nabla A\right)_i = \sum_j m_j \frac{8}{(\rho_i + \rho_j)^2} \frac{A_{ij}\mathbf{r}_{ij} \cdot \nabla_i W_{ij}}{|\mathbf{r}_{ij}^2| + \eta^2} \tag{10}$$

where $A_{ij} = A_i - A_j$, $\mathbf{r}_{ij} = \mathbf{r}_i - \mathbf{r}_j$ and η is a small number introduced to avoid a zero denominator during computations and is set to 0.1 h.

3. Governing equations

The governing equations for transient compressible fluid flow include the conservation of mass and momentum equations. In a Lagrangian framework these can be written as:

$$\frac{1}{\rho}\frac{D\rho}{Dt} + \nabla \cdot \mathbf{v} = 0 \tag{11}$$

$$\frac{D\mathbf{v}}{Dt} = \mathbf{g} + \frac{1}{\rho}\nabla \cdot \tau - \frac{1}{\rho}\nabla P \tag{12}$$

where t is time, $\mathbf{g}$ is the gravitational acceleration, P is pressure, $\mathbf{v}$ is the velocity vector and D/Dt refers to the material derivative. The density ρ has been intentionally kept in the equations to be able to enforce the incompressibility of the fluid. Using an appropriate constitutive equation to model the shear stress tensor τ, one can use equations (11) and (12) to solve both Newtonian and non-Newtonian flows.

The momentum equations include three driving force terms, i.e. body force, forces due to divergence of stress tensor and the pressure gradient. These must be handled along with the incompressibility constraint. In a SPH formulation the above system of governing equations must be solved for each particle at each time-step. The sequence with which the force terms are incorporated can be different from one algorithm to another. In the rest of this section treatment of viscous terms are explained and the models used in this paper for non-Newtonian fluid flows are briefly described.

3.1 Viscous terms

In the context of SPH method, several forms of viscosity terms were presented by Lucy (1977), Wood (1981), Monaghan and Gingold (1983) and Loewenstein and Mathews (1986). One of the most commonly used of such forms is obtained by writing the momentum equation as (Schlatter, 1999):

$$\frac{D\mathbf{v}}{Dt} = -\sum_j m_j \left(\frac{P_i}{\rho_i^2} + \frac{P_j}{\rho_i^2} + \prod_{ij} \right) \nabla_i W_{ij} \tag{13}$$

The main purpose of adding the artificial viscosity term $\prod_{ij}$ was to model strong shocks in astrophysical processes (Benz *et al.*, 1990; Monaghan, 1992). Morris *et al.* (1997) found that if this form is used to model real viscous terms, it may produce inaccurate velocity profiles in some situations.

As the purpose of this work is to solve non-Newtonian fluid flows, a new description of viscosity is presented that facilitates modeling of such flow problems. Generally speaking, viscosity of incompressible generalized Newtonian fluids depends only on the second principal invariant of the shear strain rate $\mathbf{D} = (\nabla \mathbf{v} + \nabla \mathbf{v}^T)/2$, i.e. (Vola *et al.*, 2004):

$$|\mathbf{D}| = \sqrt{\sum_{i,j} \mathbf{D}_{ij}\mathbf{D}_{ij}} \tag{14}$$

In two-dimensions, assuming $\mathbf{v} = u\mathbf{i} + v\mathbf{j}$, one gets:

$$\mathbf{D} = \frac{1}{2}(\nabla\mathbf{v} + \nabla\mathbf{v}^{\mathrm{T}}) = \begin{bmatrix} \frac{\partial u}{\partial x} & \frac{1}{2}\left(\frac{\partial u}{\partial y} + \frac{\partial v}{\partial x}\right) \\ \frac{1}{2}\left(\frac{\partial u}{\partial y} + \frac{\partial v}{\partial x}\right) & \frac{\partial v}{\partial y} \end{bmatrix} \tag{15}$$

A classical constitutive law for these generalized Newtonian fluids is given by (Vola *et al.*, 2004):

$$\tau = \mu(|\mathbf{D}|)\mathbf{D} \tag{16}$$

This formulation can also handle visco-plastic fluids but special care should be given as a multi-valued expression is normally used for such cases. For Newtonian fluids the familiar form $\tau = 2\mu\mathbf{D}$ is recovered.

Typical derivatives which appear in equation (15) can be evaluated in the SPH context as:

$$\left(\frac{\partial u}{\partial x}\right)_i = \sum_j \frac{m_j}{\rho_j}(u_j - u_i)\frac{x_i - x_j}{|\mathbf{r}_{ij}|}\frac{\mathrm{d}W}{\mathrm{d}\mathbf{r}_{ij}} \tag{17}$$

$$\left(\frac{\partial u}{\partial y}\right)_i = \sum_j \frac{m_j}{\rho_j}(u_j - u_i)\frac{y_i - y_j}{|\mathbf{r}_{ij}|}\frac{\mathrm{d}W}{\mathrm{d}\mathbf{r}_{ij}} \tag{18}$$

where $\mathbf{r}_{ij} = \mathbf{r}_i - \mathbf{r}_j$. Other derivatives can be calculated in the same fashion. Consequently, the stress tensor (τ) can be calculated for any specified constitutive law. In this work, the divergence of the stress tensor in the momentum equation is obtained as:

$$\left(\frac{1}{\rho}\nabla\cdot\tau\right)_i = \sum_j m_j\left(\frac{\tau_{\mathbf{i}}}{\rho_i^2} + \frac{\tau_{\mathbf{j}}}{\rho_i^2}\right)\nabla_i W(\mathbf{r}_{ij}, h) \tag{19}$$

where:

$$\nabla_i W(\mathbf{r}_{ij}, h) = \frac{\mathrm{d}W}{\mathrm{d}\mathbf{r}_{ij}}\frac{1}{|\mathbf{r}_{ij}|}[(x_i - x_j)\mathbf{i} + (y_i - y_j)\mathbf{j}] \tag{20}$$

It is noted that the dot product of the second order tensor τ and the vector ∇W is a vector.

Below three different non-Newtonian fluid models of interest in this work are described.

3.1.1 Power-law model. The shear stress tensor in the power-law model is expressed by (Vola *et al.*, 2004):

$$\tau = 2\mu|\mathbf{D}|^{N-1}\mathbf{D} \tag{21}$$

where N is a model exponent parameter.

3.1.2 Bingham-plastic model. The visco-plastic fluids have an "un-sheared" or "solid" zone under their yield stress point and their constitutive law represents a multi-valued function. In fact, under their yield stress point τ_Y they behave like a solid

and above this point they behave like a Newtonian fluid with constant viscosity. The constitutive law for these fluids is given by:

$$|\tau| \leq \tau_Y \rightarrow \mathbf{D} = 0 \tag{22}$$

$$|\tau| > \tau_Y \rightarrow \tau = \left(\frac{\tau_Y}{|\mathbf{D}|} + 2\mu\right)\mathbf{D} \tag{23}$$

In this paper, the solid zone is approximated via a highly viscous fluid whose viscosity is much (say, $\alpha = 100$ times) greater than the main fluid. This condition is used as long as stress is below the yield value, that is, $2\alpha\mu|\mathbf{D}| \leq \tau_Y$. Above this limit, the following relations are used:

$$|\mathbf{D}| \leq \frac{\tau_Y}{2\alpha\mu} \rightarrow \tau = 2\alpha\mu\mathbf{D} \tag{24}$$

$$|\mathbf{D}| > \frac{\tau_Y}{2\alpha\mu} \rightarrow \tau = \left(\frac{\tau_Y}{|\mathbf{D}|} + 2\mu\right)\mathbf{D} \tag{25}$$

In fact, $|\mathbf{D}|$ is calculated according to the gradient of velocity for each particle at each time-step and then it is used in the above criterion.

3.1.3 Herschel-Bulkley model. The constitutive law for the Herschel-Bulkley model is given by:

$$|\tau| \leq \tau_Y \rightarrow \mathbf{D} = 0 \tag{26}$$

$$|\tau| > \tau_Y \rightarrow \tau = \left(\frac{\tau_Y}{|\mathbf{D}|} + 2\mu|\mathbf{D}|^{N-1}\right)\mathbf{D} \tag{27}$$

It can be seen that the Bingham-plastic and the power-law models are two limit cases of this model. In the case of $N < 1$, this formulation can simulate pseudo-plastic fluids and for $N > 1$ it represents dilatant fluids. For this model, treatment of un-sheared zone is similar to the Bingham-plastic model. But above the yield point, the model resembles the power-law fluids. In a similar fashion to the Bingham model, the multi-valued constitutive law for the Herschel-Bulkley Model is implemented as:

$$|\mathbf{D}| \leq \left(\frac{\tau_Y}{2\alpha\mu}\right) \rightarrow \tau = 2\alpha\mu\mathbf{D} \tag{28}$$

$$|\mathbf{D}| > \left(\frac{\tau_Y}{2\alpha\mu}\right) \rightarrow \tau = \left(\frac{\tau_Y}{|\mathbf{D}|} + 2\mu|\mathbf{D}|^{N-1}\right)\mathbf{D} \tag{29}$$

Having computed the stress tensor τ, its divergence can be estimated by equation (19) and the momentum equations can be solved.

4. Solution algorithm

In this section, an algorithm is presented to show the sequence of computation of each term in the governing equations. In this paper, a fully explicit three-step algorithm is used. In the first step of this algorithm, the momentum equation is solved in the presence of the body forces neglecting all other forces. As a result, an intermediate velocity is computed as:

$$u^* = u_{t-\Delta t} + g_x \Delta t \tag{30}$$

$$v^* = v_{t-\Delta t} + g_y \Delta t \tag{31}$$

where $\mathbf{g} = (g_x, g_y)$ represents the gravity acceleration. Our experience has shown that it is important to impose the body forces in the first step of the solution algorithm especially in highly viscous fluids. In the second step, the calculated intermediate velocities are employed to compute $|\mathbf{D}|$ followed by the computation of divergence of the stress tensor. Note that the divergence of the stress tensor is a vector $\mathbf{S}$ given by:

$$\left(\frac{1}{\rho}\nabla \cdot \tau\right)_i = \mathbf{S} = S_x \mathbf{i} + S_y \mathbf{j} \tag{32}$$

At the end of the second step, the velocity components of each particle is updated according to:

$$u^{**} = u^* + S_x \Delta t = u_{t-\Delta t} + g_x \Delta t + S_x \Delta t \tag{33}$$

$$v^{**} = v^* + S_y \Delta t = v_{t-\Delta t} + g_y \Delta t + S_y \Delta t \tag{34}$$

At this stage, each particle is moved according to its intermediate velocity (u^{**} v^{**}) and therefore its intermediate position is given by:

$$x^* = x_{t-\Delta t} + u^{**} \Delta t \tag{35}$$

$$y^* = y_{t-\Delta t} + v^{**} \Delta t \tag{36}$$

Thus, far, no constraint has been imposed to satisfy the incompressibility of the fluid and it is expected that the density of some particles change during this updating. In fact, with the help of the continuity equation one can calculate the density variations of each particle as:

$$\frac{D_{\rho i}}{D_t} = \sum_j m_j (\mathbf{v}_i - \mathbf{v}_j) \nabla_i W(\mathbf{r}_{ij}, h) \tag{37}$$

where ρ_i and $\mathbf{v_i}$ are the density and velocity of particle i. When two particles approach each other, their relative velocity and therefore the gradient of kernel function become negative, so $D_{\rho i}/Dt$ will be positive and ρ_i will increase. Consequently, this will produce a repulsive force between the approaching particles. In a similar fashion, if two particles are repulsed from each other, an attractive force will be produced to stop this. This interaction based on the relative velocity of particles and the resulting coupling between the pressure and density will enforce incompressibility in the solution procedure.

The velocity field ($\hat{\mathbf{v}} = (\hat{\mathbf{u}}, \hat{\mathbf{v}})$) which is needed to restore the density of particles to their original value is now calculated. To do this, in the third step of the algorithm, the momentum equation with the pressure gradient term as a source term is combined with the continuity equation (11) as:

$$\frac{1}{\rho_0} \frac{\rho_0 - \rho^*}{\Delta t} + \nabla \cdot \hat{\mathbf{v}} = 0 \tag{38}$$

$$\hat{\mathbf{v}} = -\left(\frac{1}{\rho^*}\nabla P\right)\nabla t \tag{39}$$

to obtain the following pressure Poisson equation:

$$\nabla\left(\frac{1}{\rho^*}\nabla P\right) = \frac{\rho_0 - \rho^*}{\rho_0 \Delta t^2} \tag{40}$$

Equation (40) can be discretized according to equation (10) to obtain the pressure of each particle as:

$$P_i = \left(\frac{\rho_0 - \rho^*}{\rho_0 \Delta t^2} + \sum_j \frac{8m_j}{(\rho_i + \rho_j)^2} \frac{P_j \mathbf{r}_{ij} \cdot \nabla_i W_{ij}}{|\mathbf{r}_{ij}|^2 + \eta^2}\right)\left(\sum_j \frac{8m_j}{(\rho_i + \rho_j)^2} \frac{\mathbf{r}_{ij} \cdot \nabla_i W_{ij}}{|\mathbf{r}_{ij}|^2 + \eta^2}\right)^{-1} \tag{41}$$

Using equation (41) for the pressure of each particle, one can calculate $\hat{\mathbf{v}}$ according to equations (39) and (8) as:

$$\hat{\mathbf{v}}_i = -\Delta t \sum_j m_j \left(\frac{P_i}{\rho_i^{*2}} + \frac{P_j}{\rho_j^2}\right)\nabla_i W_{ij} \tag{42}$$

Finally, the velocity of each particle at the end of time-step will be obtained as:

$$u_{t+\Delta t} = u^{**} + \hat{u} \tag{43}$$

$$v_{t+\Delta t} = v^{**} + \hat{v} \tag{44}$$

and the final position of particles are calculated using a central difference scheme in time:

$$x_t = x_{t-\Delta t} + \frac{\Delta t}{2}(u_t + u_{t-\Delta t}) \tag{45}$$

$$y_t = y_{t-\Delta t} + \frac{\Delta t}{2}(v_t + v_{t-\Delta t}) \tag{46}$$

This completes the computations required for one time-step. The procedure should be repeated for every other time-step till a desired time is reached.

4.1 Boundary conditions

There are several methods for modeling boundary conditions. Monaghan proposed to cover solid boundaries with boundary particles which have 1/2 or 1/3 of the initial spacing between the particles (Monaghan, 1992). For these boundary particles the continuity and momentum equations are not solved. Boundary particles exert repulsive forces on the fluid particles to prevent them from crossing the solid boundaries. A second method assumes that solid walls act like a mirror. Therefore, if a particle approaches a solid boundary its image also does so creating an equal force but in opposite direction prohibiting the particle to penetrate the solid wall. In this work, the method proposed by Koshizuka *et al.* (1995) is used where the solid wall boundaries

are represented by fixed wall particles. These wall particles behave entirely similar to the inner particles and contribute to the solution procedure like others. So, the Poisson equation (40) is also solved for these wall particles to calculate the increasing pressure due to the approaching inner particles. Again, this increased pressure prevents the inner particles to penetrate the solid boundaries. Velocities of wall particles are set to zero at the end of each time-step to simulate a fixed wall. In this way, the wall particles correctly resemble the no-slip condition.

No especial treatment was applied on free surface particles in the computational domain. In fact, in the SPH method free surface is modeled naturally and this is one of the main advantages of the method.

4.2 Determination of time-step size

Like other CFD approaches, the SPH method requires a reasonable number of particles to achieve accurate results. Stability analysis is normally used to find the safe time-step values. In this work, the time-step Δt is calculated so that it satisfies the following Courant condition (Shao and Lo, 2003):

$$\Delta t \leq 0.1 \frac{h}{V_{\max}} \tag{47}$$

where $V_{\max}$ is the maximum particle velocity in the computation. The factor 0.1 ensures that the particle moves only a fraction (in this case 0.1) of the particle spacing (h) per time-step. Another constraint on the time-step comes from considering an explicit finite difference method simulating a diffusion problem. This gives the following limit on the time-step:

$$\Delta t \leq \beta \frac{h^2}{\mu_{\text{eff}}/\rho} \tag{48}$$

where β is a coefficient depending on the choice of the kernel type and particle arrangement. β is usually found by numerical experiments and is of order 0.1. The effective viscosity μ_{eff} is calculated according to a simple Newtonian model. Obviously the allowable time-step should satisfy both of the above criteria.

5. Test cases

In this section, three benchmark problems are studied to demonstrate the capability of the proposed algorithm to solve non-Newtonian fluid flow problems. The first problem involves free surface flow while the second problem deals with a confined flow problem. Finally, the third test case involves interface between two fluids, a Newtonian fluid and a non-Newtonian fluid.

5.1 The two-dimensional broken dam problem

The sudden collapse of a column of fluid on a horizontal surface, the so-called broken dam problem, is a classical benchmark problem for assessment of free surface modeling techniques. As shown in Figure 1, the problem consists of a rectangular ($H \times L$) column of fluid confined between a fixed wall and a temporary wall (dam) and a mild slope. At time $t = 0$, the dam is removed allowing the fluid column to collapse under the influence of gravity.

Here, the problem is solved for both Newtonian and non-Newtonian fluids. Komatina and Jovanovic (1997) obtained the experimental data for the collapse of a

water-clay mixture. In their study, the slope of the channel bed was 0.1 percent with an initial column height of $H = 0.1$ m and an initial column width of $L = 2.0$ m. For the Newtonian fluid, pure water is used while for the non-Newtonian fluid model the volume concentration of the mixture is 27.4 percent which corresponds to a density of $\rho = 1{,}200\,\text{kg/m}^3$. The rheological parameters for various fluid models used in this study are given in Table I.

In this simulation particles are used in a structural pattern with an initial spacing $L_0 = 5$ mm, so that a set of 20 × 400 particles is employed.

In Figure 2 the non-dimensional surge front positions of the collapsing dam are plotted against the non-dimensional time $t/\sqrt{H/g}$ for various models including Newtonian and three non-Newtonian fluids. The results obtained by

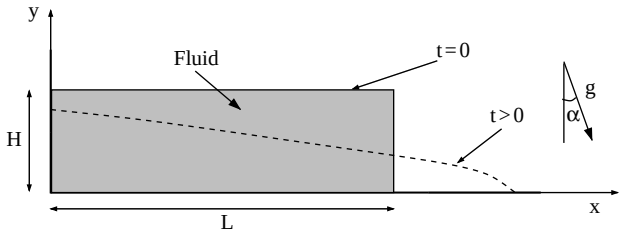

Figure 1.
Schematic of the breaking dam problem

Table I.
Rheological parameters for Broken-dam problem

Water	Power-law	Bingham plastic	Herschel-Bulkley
$\mu = 0.001$	$N = 0.15$, $\mu = 1.74$	$\tau_y = 25$, $\mu = 0.07$	$N = 0.4$, $\tau_Y = 3.5$, $\mu = 0.25$

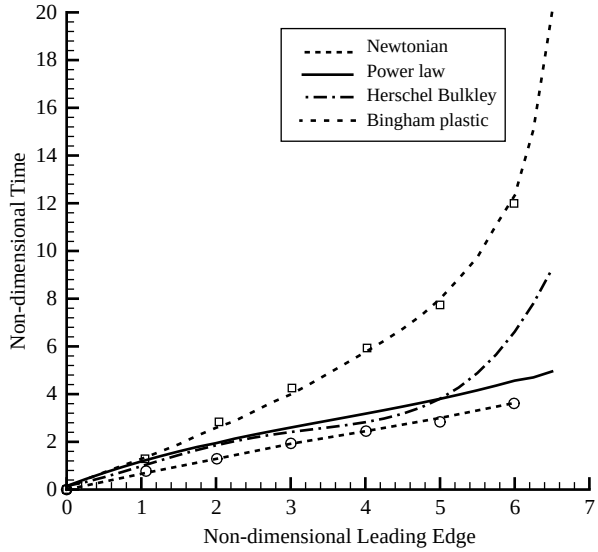

Source: Symbols show results of Komatina and Jovanovic (1997)

Figure 2.
Non-dimensional surge front for Newtonian and various non-Newtonian models

Komatina and Jovanovic (1997) are also shown in the same figure. A close agreement is observed between the experimental results and those obtained by the proposed method. Figure 3 shows the shape of the free surface at various times.

5.2 Annular viscometer

In this test case, the tangential creeping flow in a viscometer made of two coaxial cylinders is studied. As shown in Figure 4, the outer cylinder is kept fixed while the inner cylinder rotates with a constant angular velocity $\omega = 1(1/s)$. Depending on the rheological properties of the fluid, an analytical solution for this problem can be found. For the power-law model the tangential velocity is given by (Bird *et al.*, 1987):

$$u_\theta(r) = r\omega\left[\left(\frac{R_0}{r}\right)^{2/N} - 1\right]\left[\left(\frac{R_0}{R_i}\right)^{2/N} - 1\right]^{-1} \tag{49}$$

When yield stress is involved in a fluid model, a rigid zone might appear near the outer cylinder while the rest of the fluid behaves like a viscous sheared material. The radius at which transition from solid to sheared zone occurs can be found for certain values of the exponent N. For a Bingham fluid (Bird *et al.*, 1987), the transition radius R_i is obtained from:

$$\left(\frac{R_1}{R_i}\right)^2 - 2\ln\left(\frac{R_1}{R_i}\right) - \left(\frac{2\sqrt{2}\mu\omega}{\tau_Y} + 1\right) = 0 \tag{50}$$

Then, the tangential velocity in the sheared zone, is calculated according to the following equation:

$$u_\theta(r) = r\frac{\sqrt{2}\tau_Y}{4\mu}\left[\left(\frac{R_1}{r}\right)^2 - 2\ln\left(\frac{R_1}{r}\right) - 1\right] \tag{51}$$

For a pseudo-plastic Herschel-Bulkley fluid, with $N = 0.5$, the transition radius R_1 is solution of:

$$\left(\frac{R_1}{R_i}\right)^4 - 4\left(\frac{R_1}{R_i}\right)^2 + 4\ln\left(\frac{R_1}{R_i}\right) - \left(\frac{8\sqrt{2}\mu^2\omega}{\tau_y^2} - 3\right) = 0 \tag{52}$$

and the tangential velocity in the sheared zone becomes:

$$u_\theta(r) = r\frac{\sqrt{2}\tau_Y^2}{4\mu^2}\left[\frac{3}{4} + \frac{R_1^4}{4r^4} - \frac{R_1^2}{r^2} + \ln\left(\frac{R_1}{r}\right)\right] \tag{53}$$

5.2.1 Particle placement. Using different particle spacing in SPH is equivalent to using different approximation orders in the discretization method. It is common in SPH to arrange particles initially in a square pattern. In the present problem, however, as the boundary has a circular shape, filling the domain with a square arrangement results in the creation of sharp edges on the boundary. The particles at the sharp edges have less neighboring particles thus are prone to generation of numerical errors which can amplify. As momentum diffuses into the domain from the boundary particles, the

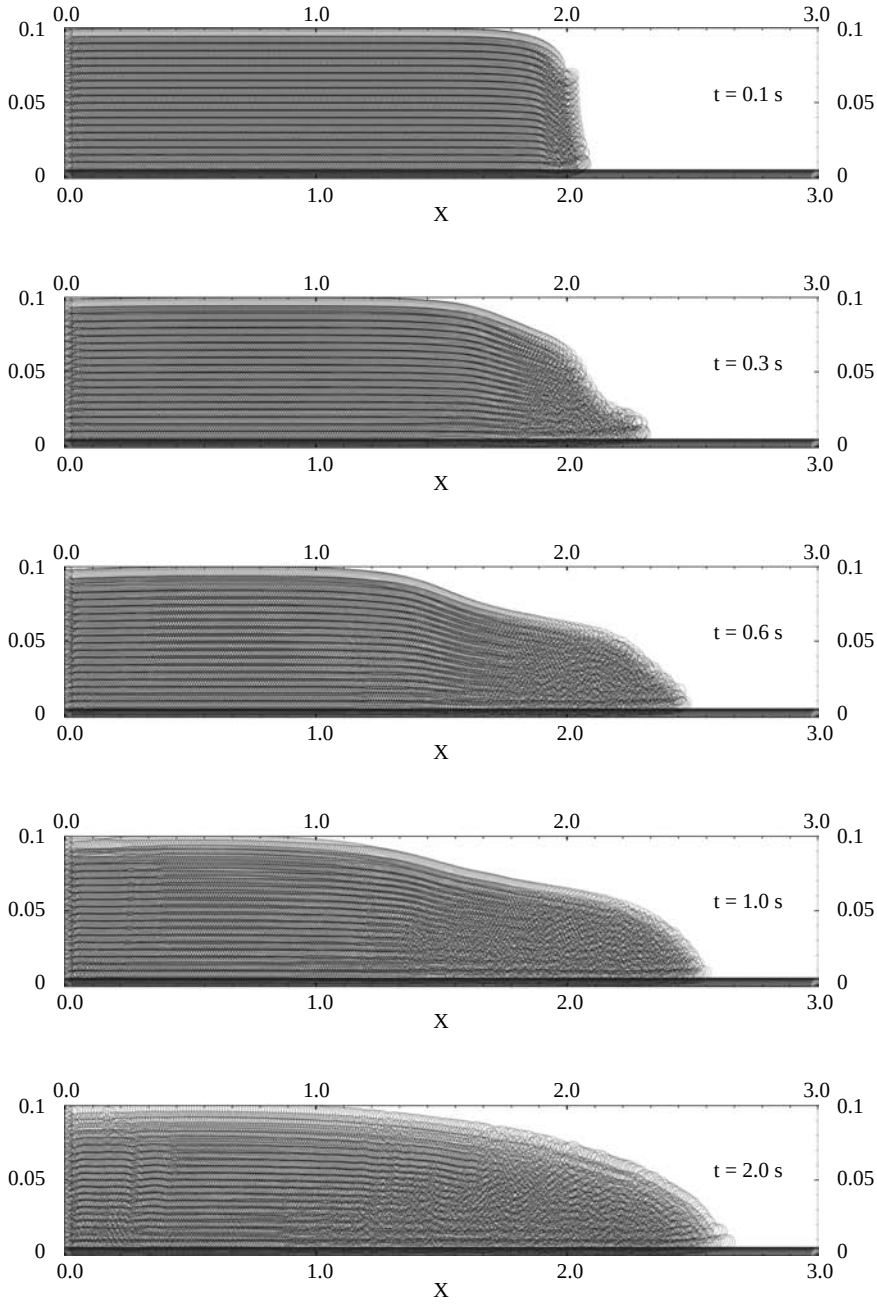

Figure 3.
Shape of free surface at various times

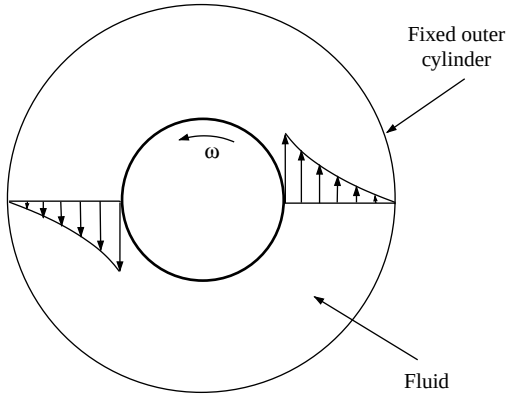

Figure 4.
Schematic of annular viscometer problem

presence of these boundary particles are significant and can delay the convergence. To control this problem, it is required to decrease the time-step size. It is important that the initial spacing between the particles must be nearly uniform. If in certain regions the initial spacing is less than the other regions, it means that the particle density is not uniform in the domain. To satisfy this condition, particles are placed on equi-centered circles of a difference L_0 (the initial spacing between particles) between their radii. The tangential spacing of the particles on each circle is also L_0. As L_0/R becomes smaller, the approximation becomes better.

Figure 5 shows the results obtained using the present SPH method ($L_0 = 25\,\text{mm}$) with the analytical solutions available for each case. It is seen that for this case the solution is in close agreement with the analytical solution.

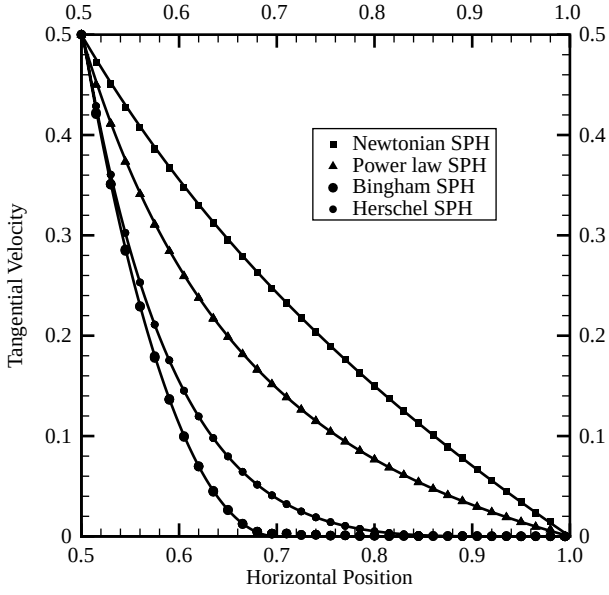

Figure 5.
Comparison of computed tangential velocities (symbols) for various models with analytical solutions (lines)

5.2.2 Convergence study. It is expected that by decreasing the initial spacing of the particles or increasing the number of particles the accuracy of the solution is increased. To achieve a particle spacing independent solution, the spacing was systematically reduced till further reduction does not alter the solution. For each case, the spacing was reduced in three steps. Figure 6 shows a typical convergence study and as can be seen the solution for $L_0 = 15$ and $L_0 = 10$ are almost the same.

5.3 Gravity current of fluid mud on sloping bed

As a final test case, laminar gravity current of fluid mud on a mild inclined bed is studied. The set up of this problem is shown in Figure 7 where all dimensions are in meters and the bed slope is 1: 40. The actual laboratory flume used for the experiment by Van Kessel and Kranenburg (1996) is 0.5 m wide. The mud fluid is represented by a suspension of China-clay in tap water whose bulk density is 1,200 kg/m^3. The flume is filled with tap water and is separated from the suspension compartment by a movable weir. When the hydrostatic pressure of the suspension at the bottom of the inflow compartment is equal to that of the tap water in the flume, the weir is lifted up to the desired height, i.e. 5 cm. The water level in the flume is kept constant by means of an overflow weir. The flow rate was kept constant, i.e. 0.004 m^3/s.

Van Kessel and Kranenburg presented experimental data for this problem and also derived an analytical solution assuming Bingham plastic rheological model for the fluid mud. They neglected sediment settling and also argued that the interfacial shear stress between the mud layer and the overlying water can be neglected.

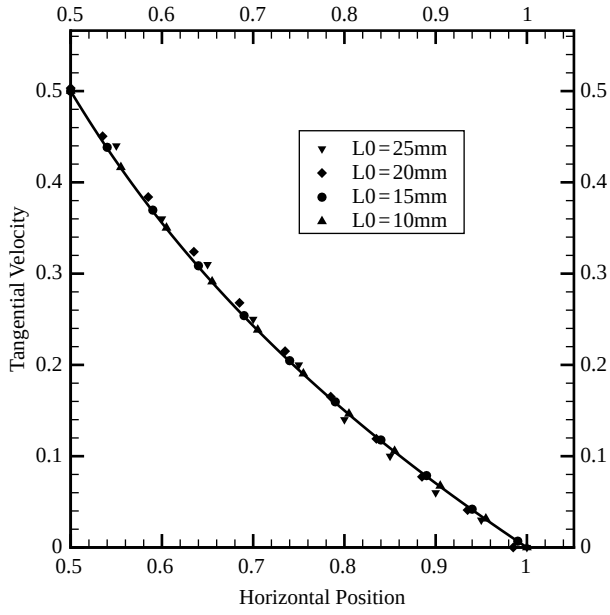

Figure 6.
Effect of particle spacing on the accuracy

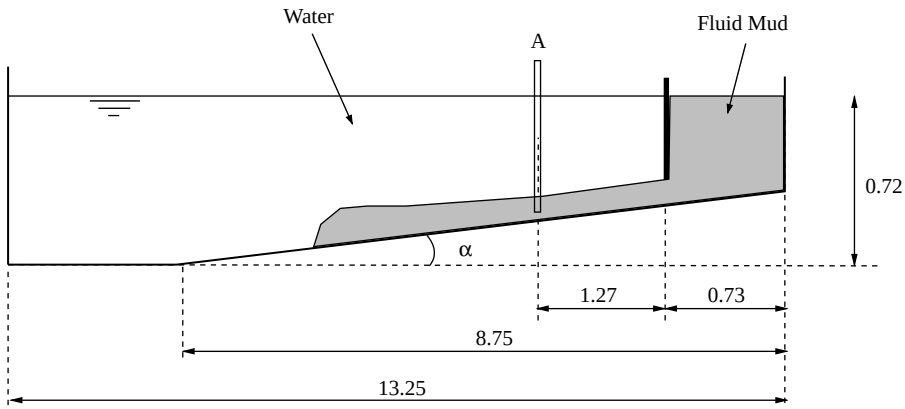

Figure 7.
Definition of the problem

The rheological behavior of the suspension is modeled as a Bingham plastic as defined by equation (22). The following empirical correlations are used for τ_Y and μ:

$$\tau_Y = c_1 N^{C_2} \quad \mu = \mu_\omega (1 + c_3 N^{c_4}) \tag{54}$$

where N is the volumetric concentration of clay defined by:

$$N = \frac{\rho - \rho_\omega}{\rho_s - \rho_\omega} \tag{55}$$

where ρ, ρ_s and ρ_w are bulk density of suspension, density of China-clay sediment (2,590 kg/m^3) and density of water. Van Kessel and Kranenburg suggested to use $c_1 = 832$ Pa, $c_2 = 3$, $c_3 = 206$ and $c_4 = 1.68$. This means that the values $\tau_Y = 2.5$ Pa and $\mu \approx 9\mu_\omega$ are adopted here.

The density and velocity profiles at section A (Figure 7) with a distance 1.27 m from the weir are compared with experimental data in Figure 8. Van Kessel and Kranenburg observed that for high suspension densities ($>$1,150 kg/m^3) interfacial mixing between the suspension layer and overlying water layer is negligible. This is in agreement with the assumption made in the present computations where no entrainment mechanism was included.

The computed tangential velocity component along the slope bed is also in good agreement with that of experimental both showing a partially plug-like profile in the mud region. Figure 9 shows the progress of the mud flow along the bed at different times. The time-step for solving this problem was set to $\Delta t = 0.0005$. All computations were performed on a P4 computer with a 2.4 GHz processor. For this problem, every 35 time-step took about 10 s.

An interesting aspect of the SPH method for this particular problem is that a two-fluid system can be easily modeled and the interface between the two fluids can be captured without extra treatments. To introduce a multi-fluid system, one only requires to give proper physical properties for particles of each fluid.

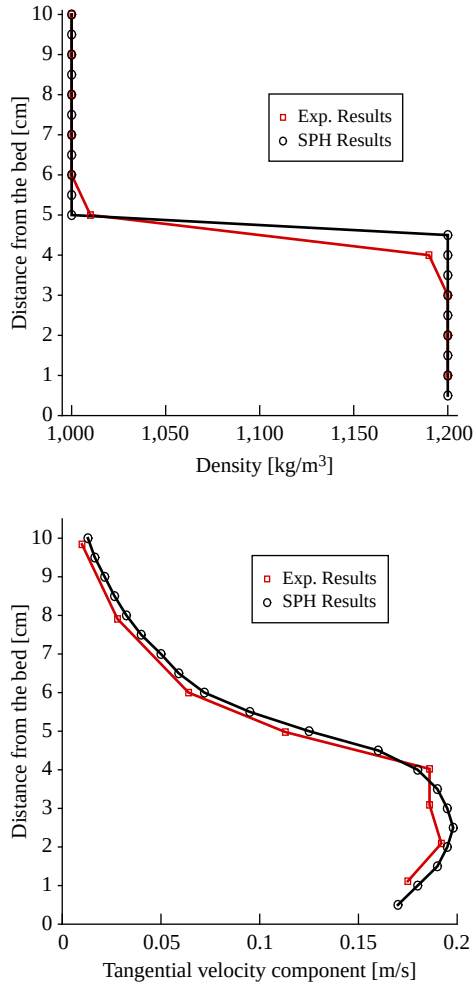

Figure 8.
Variation of density (left) and velocity (right) with distance from the bed

6. Conclusion

In this paper, a fully explicit three-step SPH algorithm was developed for simulation of incompressible Newtonian and non-Newtonian fluid flows. A new approach for computation of viscous terms was described to simplify the incorporation of shear strain for various non-Newtonian fluids. The new method of treatment of viscous terms was validated by solving three 2D test cases involving internal flow, free surface flow and interface between two fluids. Results show that the proposed method provides accurate results for all test cases solved here while requires no special treatment to deal with transition from viscous flow to solid behavior and two-fluid systems.

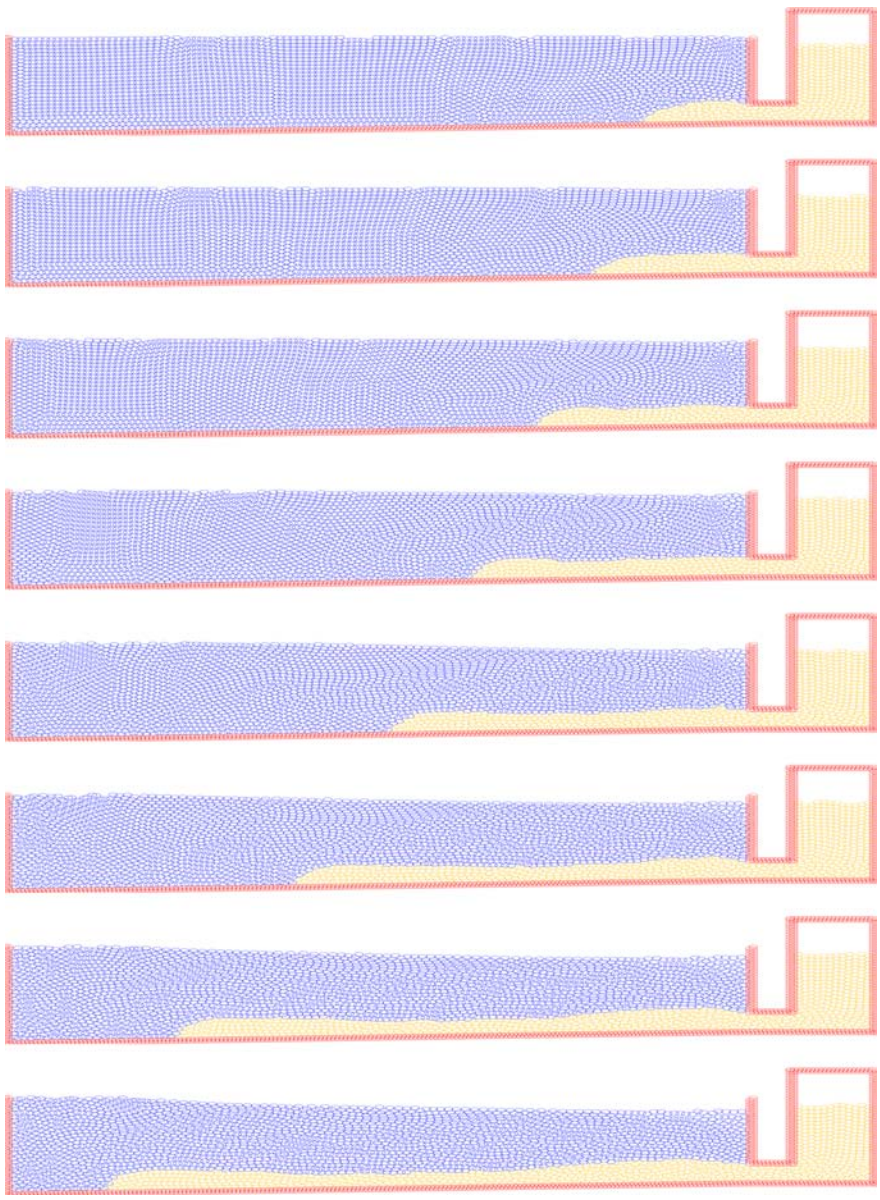

Figure 9.
Mud front at different times (from top to bottom: $t = 12, 16, 20, 24, 28, 32, 36$ and 38 (s))

References

Baaijens, F.P.T. (1998), "Mixed finite element methods for viscoelastic flow analysis: a review", *Journal of Non-Newtonian Fluid Mechanics*, Vol. 79, pp. 361-85.

Benz, W., Bowers, R.L., Cameron, A.G.W. and Press, W.H. (1990), "SPH", *Ap. J.*, Vol. 348, pp. 647-67.

Bingham, E.G. (1922), *Fluidity and Plasticity*, McGraw-Hill, New York, NY.

Bird, R.B., Armstrong, R.C. and Hassager, O. (1987), *Dynamics of Polymeric Liquids-Fluid Mechanics*, 2nd ed., Vol. 1, Wiley, New York, NY.

Bonet, J. and Lok, T.S.L. (1999), "Variational and momentum preservation aspects of smooth particle hydrodynamic formulations", *Comput. Methods Appl. Mech. Engrg.*, Vol. 180, pp. 97-115.

Bose, A. and Carey, G.F. (1999), "Least-squares p-r finite element methods for incompressible non-newtonian flows", *Comput. Methods Appl. Mech. Engrg.*, Vol. 180, pp. 431-58.

Chaniotis, A.K., Poulikakos, D. and Koumoutasakos, P. (2002), "Remeshed smoothed particle hydrodynamics for the simulation of viscous and heat conducting flows", *J. Comp. Physics*, Vol. 182, pp. 67-90.

Cleary, P., Ha, J., Alguine, V. and Nguyen, T. (2002), "Flow modelling in casting processes", *Applied Mathematical Modelling*, Vol. 26, pp. 171-90.

Colagrossi, A. and Landrini, M. (2003), "Numerical simulation of interfacial flows by smoothed particle hydrodynamics", *J. Comp. Physics*, Vol. 191, pp. 448-75.

Cummins, S.J. and Rudman, M. (1999), "An SPH projection method", *J. Comp. Physics*, Vol. 152, pp. 584-607.

Ellero, M., Kroger, M. and Hess, S. (2002), "Viscoelastic flows studied by smoothed particle hydrodynamics", *Journal of Non-Newtonian Fluid Mechanics*, Vol. 105, pp. 35-51.

Fulk, D.A. and Quinn, D.W. (1996), "An analysis of 1-d smoothed particle hydrodynamics kernels", *J. Comp. Physics*, Vol. 126, pp. 165-80.

Gingold, R.A. and Monaghan, J.J. (1977), "Smoothed particle hydrodnamics: theory and application to nonspherical stars", *Monthly Notices of the Royal Astronomical Society*, Vol. 181, pp. 275-389.

Gingold, R.A. and Monaghan, J.J. (1982), "Kernel estimates as a basis for general particle methods in hydrodynamics", *J. Comp. Physics*, Vol. 46, pp. 429-53.

Hongbin, J. and Xin, D. (2004), "On criterions for smoothed particle hydrodynamics kernels in stable field", *J. Comp. Physics*, Vol. 202 No. 2, pp. 699-709.

Kelecy, F.J. and Fletcher, R.H. (1997), "The development of a free surface capturing approach for multidimensional free surface flow in closed container", *J. Comp. Physics*, Vol. 138, pp. 939-80.

Komatina, D. and Jovanovic, M. (1997), "Experimental study of steady and unsteady free surface flows with water-clay mixtures", *J. Hydraul. Res.*, Vol. 35 No. 5, pp. 579-90.

Koshizuka, S., Nobe, A. and Oka, Y. (1998), "Numerical analysis of breaking waves using the moving particle semi-implicit method", *Int. J. Numer. Methods Fluids*, Vol. 26, pp. 751-69.

Koshizuka, S., Oka, Y. and Tamako, H. (1995), "A particle method for calculating splashing of incompressible viscous fluid", paper presented at International Conference on Mathematics and Computations, Vol. 2, pp. 1514-21.

Loewenstein, M. and Mathews, W.G. (1986), "Adiabatic particle hydrodynamics in three dimensions", *J. Comp. Physics*, Vol. 62 No. 2, pp. 414-28.

Lucy, L.B. (1977), "A numerical approach to the testing of the fission hypothesis", *Astron. J.*, Vol. 82, pp. 1013-20.

Matallah, H., Townsend, P. and Webster, M.F. (2002), "Viscoelastic computations of polymeric wire-coating flows", *Int. J. Num. Meth. Heat Fluid Flow*, Vol. 12 No. 4, pp. 404-33.

Monaghan, J.J. (1985), "Extrapolating b-splines for interpolation", *J. Comp. Physics*, Vol. 60 No. 2, pp. 253-62.

Monaghan, J.J. (1992), "Smoothed particle hydrodynamics", *Annul. Rev. Astron. Astrophys.*, Vol. 30, pp. 543-74.

Monaghan, J.J. (1994), "Simulating free surface flows with SPH", *J. Comp. Physics*, Vol. 110, pp. 399-406.

Monaghan, J.J. and Gingold, R.A. (1983), "Shock simulation by the particle method SPH", *J. Comp. Physics*, Vol. 52, pp. 374-89.

Morris, J.P., Fox, P.J. and Zhu, Y. (1997), "Modeling low Reynolds number incompressible flows using SPH", *J. Comp. Physics*, Vol. 136, pp. 214-26.

Owen, J.M. (2004), "A tensor viscosity for SPH", *J. Comp. Physics*, Vol. 201, pp. 610-29.

Owens, R.G. and Phillips, T.N. (2002), *Computational Rheology*, Imperial College Press, London.

Renardy, M. (2000), "Current issues in non-Newtonian flows: a mathematical perspective", *Journal of Non-Newtonian Fluid Mechanics*, Vol. 90, pp. 243-59.

Schlatter, B. (1999), "A pedagogical tool using smoothed particle hydrodynamics to model fluid flow past a system of cylinders", Technical Report, Oregon State University, Corvallis, OR.

Shao, S. and Lo, E.Y.M. (2003), "Incompressible SPH method for simulating Newtonian and non-Newtonian flows with a free surface", *Advances in Water Resources*, Vol. 26, pp. 787-800.

Takeda, H., Miyama, S.M. and Sekiya, M. (1994), "Numerical simulation of viscous flow by smoothed particle hydrodynamics", *Progress of Theoretical Physics*, Vol. 92 No. 5, pp. 939-60.

Van Kessel, T. and Kranenburg, C. (1996), "Gravity current of fluid mud on sloping bed", *Journal of Hydraulic Engineering*, Vol. 122 No. 12, pp. 710-6.

Vola, D., Babik, F. and Latche, J.C. (2004), "On a numerical strategy to compute gravity currents of non-Newtonian fluids", *J. Comp. Physics*, Vol. 201 No. 2, pp. 397-420.

Webster, M.F., Tamaddon-Jahromi, H.R. and Aboubacar, M. (2004), "Transient viscoelastic flows in planar contractions", *Journal of Non-Newtonian Fluid Mechanics*, Vol. 118 Nos 2/3, pp. 83-101.

Welton, W.C. (1998), "Two-dimensional PDF/SPH simulation of compressible turbulent flows", *J. Comp. Physics*, Vol. 139, pp. 410-43.

Wood, D. (1981), "Collapse and fragmentation of isothermal gas clouds", *Monthly Notices of the Royal Astronomical Society*, Vol. 194 No. 1, pp. 201-18.

Corresponding author
M.T. Manzari can be contacted at: mtmanzari@sharif.edu